J. Cardiovasc Disease Res., 2020; 11(2): 96 – 108
A Multifaceted Peer Reviewed Journal in the field of Cardiology
www.jcdronline.org | www.journalonweb.com/jcdr
P – ISSN: 0975 – 3583 Online: 0976 – 2833

Gradient Orientation Mapping Based Fuzzy C-Means Clustering for Digital Dental X-Ray Images

Peer Ahamed Buhari.M[1], Dr. S. KotherMohideen[2]
[1]Research Scholar, Department of Computer Science, Bharathiar University, Coimbatore, Tamil Nadu, India
E-mail: buhari31@gmail.com
[2]Associate Professor, HOD and Research Head, PG Department of Information Technology, Sri Ram Nallamani Yadava College of Arts and Science, Tenkasi, Tirunelveli, Tamil Nadu, India

ABSTRACT

In recent development research, the dental radiographic examination generally essential for the diagnosis of dental disorders. Various approaches are used to identify cancer cells. The proposed novel approach, called the Gradient Orientation Mapping Dependent Fuzzy C-Means (GOMB-FCM) algorithm, is being used to evaluate a dental membership function. Using a house, the metric is structured to determine the form that is unusual in dentistry. The overall accuracy of 95 per cent is achieved through the proposed GOMB-FCM process. The result, precision and consistency values for the proposed segmentation method were found to be 96.7%, 95.6% and 98.4% respectively. The similarity of the proposed solution to True Positive values in the ROC curve means that performance is higher. The comparative analysis with ResNet-50 focuses on different test and training details of 90 to 10 per cent, 80 to 20 per cent and 70 to 3 per cent, respectively, which demonstrates the robustness of the proposed research work. The preliminary results demonstrate the suggested efficiency of the system relative to other detection strategies.

Keywords: Dental X-Ray, Mix Pixels, Fuzzy C - Mean Clustering, RGB Conversion, Image Enhancement, JPEG Format, Equalization of the Histogram

Correspondence:
Peer Ahamed Buhari M
Research Scholar
Department of Computer Science
Bharathiar University
Coimbatore, Tamil Nadu, India
E-mail Address: buhari31@gmail.com

Submitted: 28-04-2020
Revision: 21-05-2020
Accepted Date: 15-06-2020

DOI: 10.31838/jcdr.2020.11.02.16

INTRODUCTION

Several picture segmentations have been introduced in recent decades to boost the efficiency of segmentation. Segmentation of dental X-ray picture plays a significant role in the study of dental X-ray images in the area of practising dentistry, such as technical assistance and identification techniques to acquire valuable information. The tooth region has a high grayscale value and is the main part of the picture. Dental building region has a medium gray colour and comprises of the structure of teeth, bones and periodontitis. The backdrop has the smallest grayscale interest among them, which reveals the history of the teeth formation. Grayscale colour variations between pixels were not important between components of dental structure such as enamel, dentin and pulp Photo segmentation is one of the most critical tasks for data recognition and image analysis, such as pattern identification and image matching. The object of segmentation is that pixels in the same field have the same quality, i.e. pixels from various areas have different values. The basic concept of a regional growth algorithm is to mix pixels with similar properties to make up a zone, i.e. for each zone to be separated, first to locate a seed pixel as a growth point and then to integrate the adjacent area with similar pixel properties in its domain. The clustering method is based on the similarity of items as the class division criteria, that is, it is divided into many subclasses according to the internal configuration of the sample collection, such that the same category of samples is as close as possible and the separate samples are not as similar as possible. The latter is a segmentation focused on weakly controlled CNN research. It relates to the problem of assigning a semantic label to every pixel in the picture and consists of three parts.1) Send the picture that contains through objects. 2) Give the boundary of the piece. (3) The location of the item in the picture is labelled with a partial marker. At present, the basic activity of the segmentation procedure is very different and nuanced from the universal imaging segmentation system, and a standardized model is not known. The segmentation of dental X-ray images is decreased as they have a magnitude of homogeneity across various parts, low picture quality due to noise and inadequate data scan contrast. This is difficult to isolate the fragments of the lip from all issues. Therefore, robust segmentation algorithms are needed to identify the X-ray dental image region. Qingyong Li et al.[1] proposed segmenting the image using a double-scale non-linear threshold for the vessel support region. It produces a fine segmentation, compared to the available methods but accuracy is less. This technique has the limitations to choose the threshold value to separate the image particles from the noisy images. To overcome these limitations, Ronghua Shang et al.[2] suggested a new image segmentation technique based on the key pixel. This approach increases overall segmentation efficiency and provides consistent production. Nonetheless, certain drawbacks render it challenging to use picture level annotations to train segmentation. Liyilei Su et al.[3] have developed an advanced, geographic and boundary-based segmentation approach for x-ray pictures. It delivers high precision. However, it focuses only on the colour of the pixels and does not bother with the other features of the graphic. To address these issues, Hong Huang et al.[4] reported a new FCM clustering algorithm based segmentation of teeth with the rough set. It functions based on homogeneous amplitude and noise-free pictures. FCM has the limitations in choosing the parameters and also detecting common boundaries among clusters. To overcome these constraints Mengxuanzhang et al. suggested an unsupervised EA-based fuzzy clustering for image segmentation, this method does not require any prior information for segmentation [5]. However, this method is not working well in noisy images because of the lack of spatial information. To overcome this an FCM segmentation with spatial constraints for medical image Segmentation proposed [6] [7]. The spatial

information derived from the images is used for the clustering process. However, there is a need for structural information and gradient information which provide better optimum segmentation at the edges. All these existing methods of segmentation has the limitations such as the fixing of the threshold value and curve function and finding the common borders of the clusters and choosing the opt parameters can be rectified by using the proposed Gradient Orientation Mapping Based Fuzzy C-Mean clustering method in which there is no need for any prior information like threshold value and curve function [15]. In this new technique, both spatial and structural information are included for segmentation and also some image features such as edge which gives the boundary of the teeth, the entropy which is used to classify the textures, intensity, Color, and Gradient features are also used to improve the performance of segmentation [17].Various segmentation concepts[19] include geographic segmentation[20], edge-based technique[21], thresholding technique[22], For the isolation of cancer cells from human cells. Various methods of classification focused on the neural network classifier [23], the SVM classifier[24] and the judgment classifier[25].Deficiencies applicable to the classification method alluded to above include inaccurate logical segmentation, decreased consistency and complicated calculations. Therefore, the various portions of the dental X-ray pictures are elegantly segmented. Scientists are focusing on increasing the precision of segmentation that can be achieved and illustrated by using this new segmentation algorithm.

PROPOSED SYSTEM

In the first example, the object of the proposed solution is to reinforce and fragment dental nodule. Finally, segmented nodules are known as dual cutting-edge approaches, the chronicles of these approaches are listed in the following sections

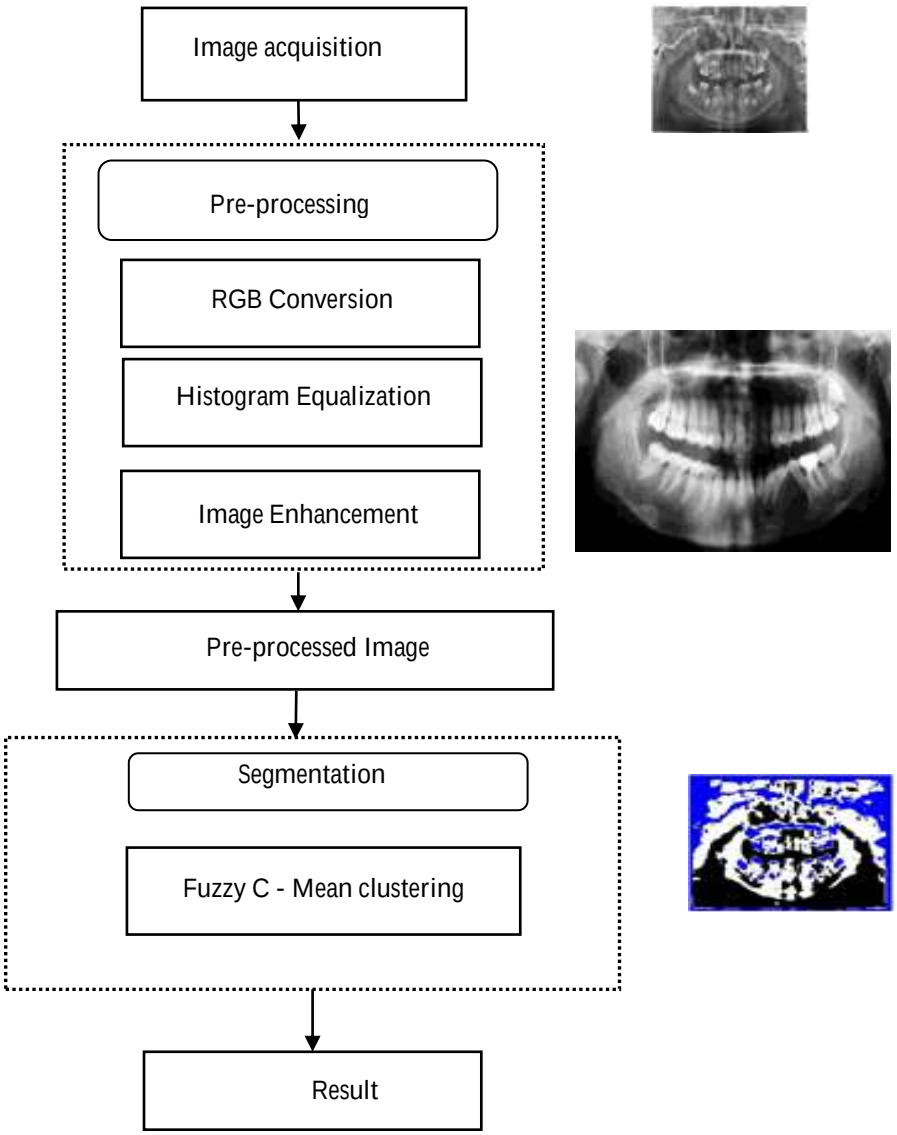

Figure 2.1: Block diagram for steps involved in the proposed approach

2.1 Image Acquisition

The planned CAD program would be introduced with the aid of MATLAB 2018a tools. MATLAB technology is used in mathematical and image recognition software. Real datasets are taken from various dental hospitals including 500 dental images during the period 2017-2019. The Publicly available dental scans of 455 patients, which include 710 nodules tested and in-house clinical dataset of 80 patients with 505 scans images exams.

2.2. Preprocessing

Pre-processing an image is an essential process for every classification since it makes the image ready for further steps. Initially, the dental image RGB colour images are converted into HSV image for the process to be simple. Colour conversion is most widely done for blending and results in colour layers that allow the product to be utilized because it primarily defines the colour mixture. Upon completion of this step, the histogram equalizes the picture {20}. Histogram equalization is added to these pre-processed pictures to improve the pixel accuracy of the photos by measuring the pixel size for these reference images, and the brightness correction together with the contrast distribution is the phase used for image processing. A global analysis of cancer dental photos with an increase in intensity values has been established.

Equalization of the histogram

Histogram equalization is a method used for image analysis and contrast adjustment utilizing the format histogram. Histogram equalization also creates artificial results in photographs; nevertheless, it is very effective for experimental images such as infrared, satellite or x-ray pictures, frequently the same type of pictures on which false-colour is added. Equalization of histograms may also generate undesirable results when applied to images with low colour depth [16].

The algorithm for the Image Equalization of the Proposed Histogram is given below:

1. Develop a picture histogram.
2. Convert the input image to a grayscale image.
3. Find the frequency of occurrence for each pixel value, i.e. the image histogram.
4. Calculate the average brightness of all pixels.

$$cdf(x) = \sum_{j=1}^{x} h(j) \qquad (2.1)$$

1. Divide the cumulative frequencies by the total number of pixels and multiply them by maximum gray count (pixel value) in the image.
2. Calculate new values using the standard histogram equalization rule.

$$eh(i) = round(\frac{cdf(1) - cdf_{\min}}{M \times N - cdf_{\min}} * (L-1)) \qquad (2.2)$$

2. Assign new values to the gray colour in the picture.
   Get a histogram and a composite histogram for the new file.
   OutputIm= histoeq (NbinsImputImage, minvalue, maximum value, displa (2.3)

3. The current pixel level value (k) is determined for increasing of the brightness values in the original picture as seen in Equation
   (3.4).$k = \sum_{i=0}^{j} {}^{N_i}/_{T}$ (2.4)
   The cumulative pixel count is where the aggregate determines the amount of pixels by calculating the combination of the histogram with the brightness of less than the words j and T.

Proposed Segmentation methods

Most specifically, picture segmentation is the method of assigning a label to each pixel in an image such that pixels with the same label share similar characteristics. After the pre-processing method, the performance of this stage is supplied to the segmentation techniques used to remove the cancerous area from dental photographs. In medical imaging, sections also apply to different forms of cells, tissues, pathologies or biologically linked structures.This type of dental segmentation is seen in low contrast increasing noise factors and another set of imaging ambiguities in terms of the function associated with the Gradient Orientation Mapping Dependent Fuzzy C-Means algorithm segmentation process, the Maximized MRF function refers to the identification of the character values concerning the labels in the picture. This clustering technique is very efficient in identifying clusters of pixels. Adaptive Regularized kernel centred Fuzzy C-Mean algorithm is the starting point for the proposed solution. Assign a pixel type to the cluster corresponding to the image, which reduces the mean distance between the assigned pixel and the centre of the cluster. The Proposed Gradient Orientation Mapping Based Fuzzy C-Means algorithm segmentation is used to calculate the minimum region threshold values based on the prior knowledge of the captured sequence of the image. This is used to stretch the

borders of the field in the foreground pixels. The picture may be segmented according to the form and the characteristics of the item. Therefore, many computerized segmentation methods have been developed for medical image computing. Below are sampling procedures in this area, where application depends on the experience offered by clinicians for the particular mission.

Proposed Gradient orientation mapping based on a fuzzy C-Mean clustering algorithm (GOMB-FCM)

To avoid the situation corresponding to the cancerous features a new ARKFCM segmentation approach for colour imaging segmentation is proposed which overcomes the existing limitations. The proposed Gradient Orientation Mapping Based Fuzzy C-Mean clustering algorithm is mentioned below.

Input: A dental X-ray image; numbers of Clusters C; fuzzifier m=3; Threshold ε; the maximal number of iterations>0

Output: Segmented image, Cluster centres, Cluster validity indices.

The algorithm for proposed segmentation Gradient orientation mapping based fuzzy C-Mean clustering (GOMB-FCM) algorithm is given below:

Step1: Assign loop counter t=0.

Step 2: Determine the objective function of Fuzzy C-mean for the given digital dental X-ray image.

Step 3: Extract the dental features for the input image and find the objective and represent it as C_2.

Step 4: Determine the objective function of ARKFCM for the input digital dental X-ray represented as(C_{add}).

$$C_{add}(v,u) = 2\left[\sum_{i=1}^{N}\sum_{j=1}^{C}\mu_{ij}^{m}(1-k(xi,vj)) + \sum_{i=1}^{N}\sum_{j=1}^{C} ri\mu_{ij}^{m}(1-k(\overline{xi},vj))\right] \quad (2.5)$$

Step 5: Calculate C by using equation

$$C = C_1+C_2+C_{add}\rightarrow \min \quad (2.6)$$

Where C_1 is the Objective function of Fuzzy C-Means obtained from step1.

C_2 represents the dental feature information obtained from step2.

$C_{add}$is the objective function of an Adaptive Regularised Kernel-based Fuzzy C-Mean algorithm.

Step 6: $$C = \sum_{k=1}^{N}\sum_{j=1}^{C}\mu_{kj}^{m}\left\|X_k - V_j\right\|^2 + \sum_{k=1}^{N}\sum_{j=1}^{C}\mu_{kj}^{m}R_{jk}^2 + \sum_{k=1}^{N}\sum_{j=1}^{C}\mu_{kj}^{m}\left(\frac{1}{1}\sum_{1=1}^{1}w_{ik}\right) + 2\left[\sum_{i=1}^{N}\sum_{j=1}^{C}\mu_{ij}^{m}(1-k(xi,vj))\right] +$$

$$\left[\sum_{i=1}^{N}\sum_{j=1}^{C} ri\mu_{ij}^{m}(1-k(\overline{xi},vj))\right] \rightarrow \min \sum_{j=1}^{C}\mu_{kj} = 1;\ \mu_{kj}\in[0,1]; \quad (2.7)$$

Step 7: Find the Centre of the cluster by taking derivative of C and equate to zero.

Step 8: Calculate $$V_j = \frac{\sum_{k=1}^{N}(\mu_{kj}^{m} + \left|\mu_{kj} - \overline{\mu_{kj}}\right|X_k}{\sum_{k=1}^{N}(\mu_{kj}^{m} + \left|\mu_{kj} - \overline{\mu_{kj}}\right|} \quad (2.8)$$

Step 9: Find the membership matrix by using the formula

$$\mu_{kj} = \frac{-\lambda_k + 2\overline{\mu_{kj}}\left\|X_k - V_j\right\|^2}{2*(2\left\|X_k - V_j\right\|^2 + R_{jk}^2 + \frac{1}{1}\sum_{i=1}^{1}w_{ik})} \quad (2.9)$$

$$\lambda_k = \frac{\left(\sum_{j=1}^{C}\frac{\overline{\mu_{kj}}\left\|X_k - V_j\right\|^2}{(2*\left\|X_k - V_j\right\|^2 + R_{jk}^2 + \frac{1}{1}\sum_{i=1}^{1}w_{ik})} - 1\right)}{\left(\sum_{j=1}^{c}\frac{1}{2(2*\left\|X_k - V_j\right\|^2 + R_{jk}^2 + \frac{1}{1}\sum_{i=1}^{1}w_{ik})}\right)} \quad (2.10)$$

If t > 100 stop. Otherwise update t=t+1 and go to step 2.

The GOMB-FCM algorithm achieves more advantages when compared to the GOMB-FCM, ARKFCM and the FCM methods [33].

1. GOMB-FCM uses the optimal results of FCM and the dental features and also additional information from

ARKFCM so that the quality would have been better than the FCM-SC[6], EA-FCM[5]and FCM[4].

2. GOMB-FCM is very easy to implement and requires less processing time.

3. This algorithm is more effective for parameter controlling because it uses the same number of the parameter as in FCM.

C. FEATURE EXTRACTION

For feature extraction, gradient features are mainly considered where the feature values mainly depend on the threshold part of the histogram-based values. By these features, classifier classifies the disease in the lung image. The histogram can be generated to obtain the feature in Histogram based features. For gradient feature extraction provides efficient values where the features can be extracted. Here, taken 200 images for testing purpose which includes both benign and malignant stages of database images [22].

GRADIENT FEATURE EXTRACTION

From these database images, gradient feature extraction, Weber local Descriptor (WLD), Local Texon XOR Pattern, Edge intensity and Entropy and finally colour enhancement RGB features are extracted.

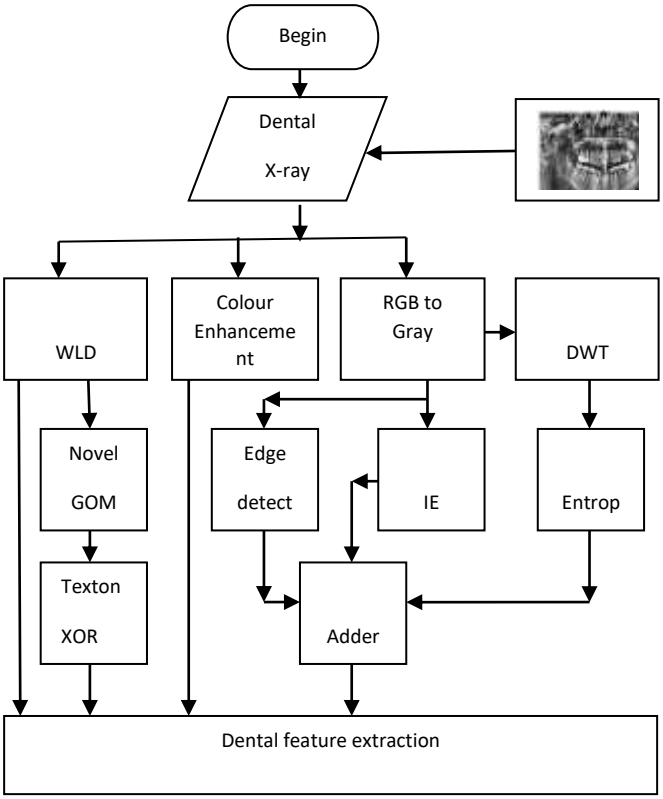

Fig 2: Dental Feature Extraction

This section shows the extraction of four dental features such as gradient features from Weber local descriptor, RGB feature, Edge Intensity Entropy features and a new improved gradient orientation mapping based feature. These features are used for further processing.

i. Weber Local Descriptor (WLD)

To obtain the gradient features of the dental X-ray image Weber Local Descriptor (WLD) which is inspired by Weber's law is used in the proposed work. WLD is a very powerful and robust local descriptor. Using the WLD features the edges can be segmented elegantly and it perform well in the context of recognition and matching because of its invariance of scaling and rotating functions [8]. These gradient features are used to separate dissimilar parts such as enamel, cementum, gum, root canal etc. It works based on the principle that the pattern of human eye perception not only depends on the change of lighting but also depends on the intensity of the light. WLD is a dense descriptor computed for every pixel and it depends on the magnitude of the centre pixel's intensity and the local intensity variation. WLD is computed using a small size filter of dimension 3 X 3. It has finer granularity.

It consists of two different components such as differential excitation and gradient orientation. Differential excitation is the ratio of the relative intensity of a current pixel (Δd_c) and its current pixel intensity (d_c). Relative intensity is the intensity variation between the current pixel intensity and its surrounding eight-pixel intensity. The relative intensity is calculated by applying filter (f_{00}) to the original image. The current pixel intensity is obtained by applying filter (f_{01}) to the original image [32].

Differential Excitation $\xi(dc) = \arctan\left(\frac{\Delta d_c}{d_c}\right)$ (2.11)

Where $\Delta d_c = \sum_{i=0}^{8} d_i - d_c$

Differential Excitation $\xi(dc) = \arctan\left(\frac{\sum_{i=0}^{8} d_i - d_c}{d_c}\right)$ (2.12)

Gradient orientation gives the local object appearance and shape of an image by the distribution of intensity gradients or edge directions.[9] The gradient orientation is the arctangent of the ratio of V_s^{11} to V_s^{10}. Where V_s^{11} is the horizontal intensity difference and it is obtained by applying filter f_{11}. V_s^{10} is the vertical intensity difference obtained by applying filter f_{10}.

Gradient orientation $\theta(dc) = \arctan\left(\frac{V_s^{11}}{V_s^{10}}\right)$ (2.13)

Where $V_s^{10} = d_5 - d_1; V_s^{11} = d_7 - d_3$

The image is further mapped from $\theta(dc) \rightarrow \theta'(dc)$ to obtain four-quadrant arctangent function.

$\theta'(dc) = \arctan 2(V_s^{11}, V_s^{10}) + \pi$ and

$$\arctan 2(V_s^{11}, V_s^{10}) = \begin{cases} \theta, & V_s^{11} > 0 \quad and \quad V_s^{10} > 0 \\ \theta + \pi, & V_s^{11} > 0 \quad and \quad V_s^{10} < 0 \\ \theta - \pi, & V_s^{11} < 0 \quad and \quad V_s^{10} < 0 \\ \theta, & V_s^{11} < 0 \quad and \quad V_s^{10} > 0 \end{cases} \quad (2.14)$$

Where $\theta \in [-\pi/2 \quad , \pi/2]$ and $\theta' \in [0 \quad , 2\pi]$

In these two components gradient orientation plays a vital role in the segmentation of teeth.

Novel gradient orientation mapping is applied to the gradient orientation feature of the dental X-ray image. The mapping pattern is shown below in equation (2.15). Using this mapping pattern ten distinct patterns are obtained from the gradient orientation feature of the digital image.

$$G(dc) = \begin{cases} 9, & \theta'(dc) \geq 90\% \ of \ M \\ 8, & \theta'(dc) \geq 80\% \ of \ M \\ 7, & \theta'(dc) \geq 70\% \ of \ M \\ 6, & \theta'(dc) \geq 60\% \ of \ M \\ 5, & \theta'(dc) \geq 50\% \ of \ M \\ 4, & \theta'(dc) \geq 40\% \ of \ M \\ 3, & \theta'(dc) \geq 30\% \ of \ M \\ 2, & \theta'(dc) \geq 20\% \ of \ M \\ 1 & \theta'(dc) \geq 10\% \ of \ M \\ 0, & \theta'(dc) < 10\% \ of \ M \end{cases} \quad (2.15)$$

Where M=Maximum intensity of the image $\theta'(dc)$

3. PERFORMANCE MEASUREMENTS

The performance of the proposed algorithm has evaluated from the measurement of Nine cluster validity indices.

Davies-Bouldin (DB)

DB index measures the average distance of elements of each cluster concerning their centroids to the distance of the centroids of the two clusters. The less value of DB provides better performance. Let $R_{i,j}$ be a measure of how good the clustering scheme.

$$DB \equiv \frac{1}{N} \sum_{i=1}^{N} D_i \quad (3.1)$$

D_i chooses the worst-case scenario, and this value is equal to $R_{i,j}$ for the most similar cluster to cluster i.

$$D_i \equiv \max_{j \neq i} R_{i,j}$$

$$Where,\ R_{i,j} = \frac{S_i + S_j}{M_{i,j}} \qquad (3.2)$$

Where $M_{i,j}$ the separation between the i^{th} and the j^{th} cluster and

S_i- cluster scatter for cluster i

RESULT AND DISCUSSION

The planned CAD framework is being developed with the aid of MATLAB 2018a tools. The MATLAB code is embedded in the statistical and image processing tools. 100 healthy and 100 malignant photographs of 345 patients from the dental archive are extracted and reviewed to achieve the segmentation and attribute extraction findings of the proposed method following steps are used to indicate the results obtained by giving the original dental image from the database. Pre-processing methods are applied to the sample images to eliminate noise and enhance the accuracy of the pictures. This move will be followed by segmenting the area from the photos. Ultimately, the corresponding features derived from the sample photos are seen in the table.

4.1 SAMPLE IMAGE

Test pictures are drawn from real dental dataset. Here the dataset photos are processed and provided to the processing CAD method. 345 patients are considered to have taken dental samples of 100 benign and 100 malignant images for this work. Figure.5.1 displays the databases of the study collected from dental photos. Any samples are taken to prove that they have been used to test the performance of the proposed device. Some dental samples are given below. Here 10 lung cancer CT scan images are retrieved from the national LIDC database and 6 CT scan images are taken from the in-house research archive.

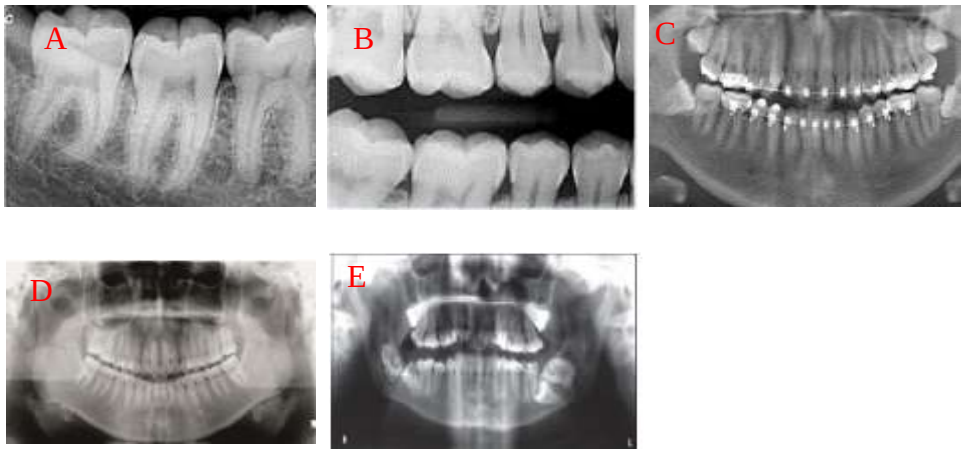

Figure 4.1: Sample data

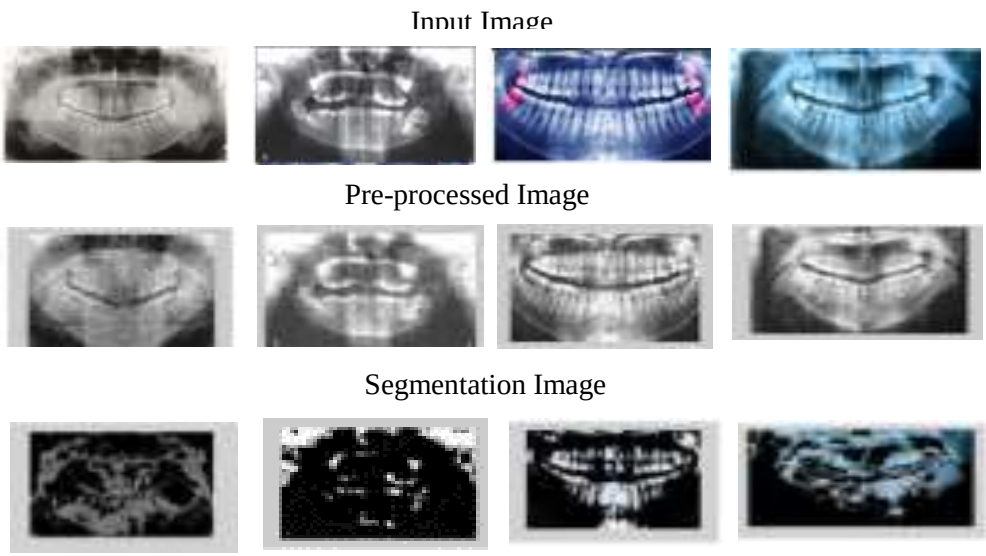

Figure 4.2: Proposed System results using CNN classifier with data set 1.

4.2 IMAGE PREPROCESSING

Pre-processing an image is an essential process for every feature extraction since it makes the image ready for further steps. Initially, the Dental image RGB colour images are converted into HSV image for the process to be simple. Colour conversion is most widely used for blending and provides colour layers that support to be included in the design because it primarily defines the colour mixture. After completion of this process, the histogram equalizes the image. Histogram equalization is added to these pre-processed images to improve the pixel accuracy of the images by determining the pixel size for these sample images, and brightness correction coupled with contrast distribution is a phrase used in image processing. The X-ray dental photographs that are translated into the JPEG format are used throughout the analysis. The photographs collected are of the same size such that there is no need to adjust the size of the file.

A) Pre-processed image of benign dental sample1 Row 1: Input Sample Image, Color Converted Image, Histogram based Equalization of image

B) Pre-processed image of malignant mental sample 2 Row 1: Input Sample Image, Color Converted Image, Histogram based Equalization of image

Figure 4.3: (a) Pre-processed image of benign dental sample 1 Row 1: Input Sample Image, Color Converted Image, Histogram based Equalization of image (b) Pre-processed image of malignant dental sample 2 Row 1: Input Sample Image, Color Converted Image, Histogram based Equalization of image.

4.3 IMAGE SEGMENTATION

After the pre-processing method, the performance of this stage is supplied to the segmentation techniques used to remove the cancerous area from dental photographs. In medical imaging, the parts typically refer to specific tissue types, tissues, pathologies or biologically related structures. In terms of the feature associated with the proposed GOMB-FCM segmentation method, the maximized MRF feature refers to the recognition of the character values concerning the labels in the image. This is used to raise the boundaries of the area in the foreground pixels. The image may be segmented by the shape and characteristics of the object.

Sl.No	Input	Otsu	FCM	ARKFCM	SSFC-SC	Proposed Method GOMB-FCM
1						

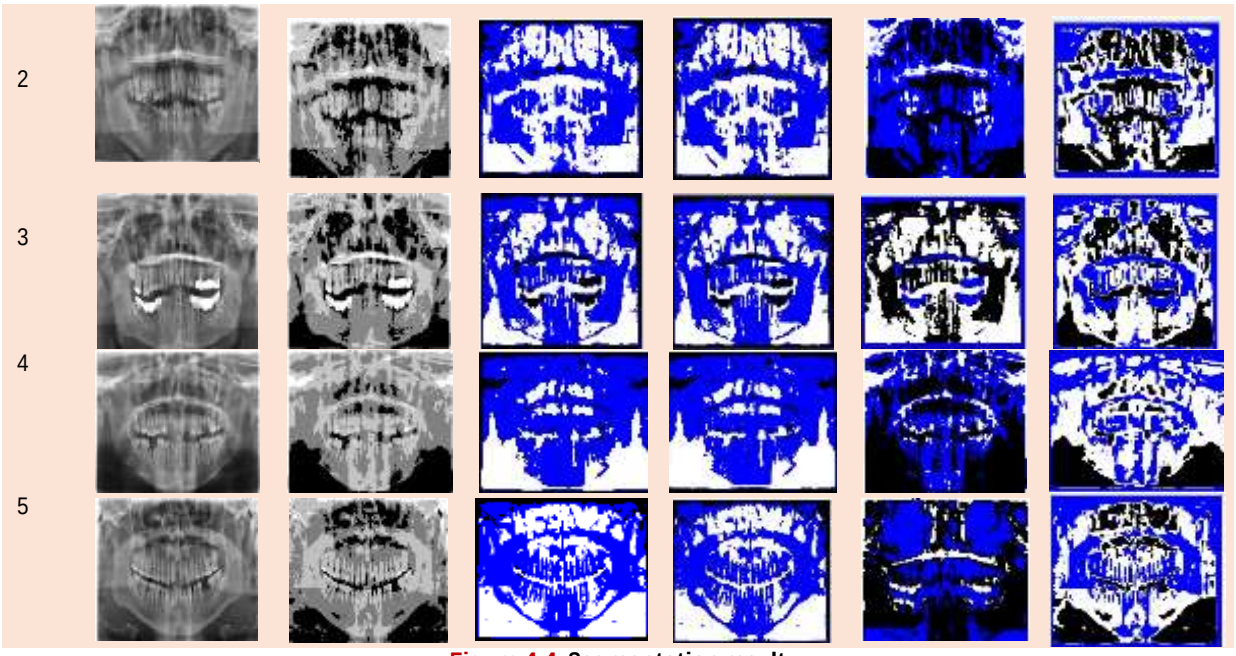

Figure 4.4: Segmentation result

Figure 4.5: GraphicalUserInterface for GOMB-FCM

The GUI for modern gradient orientation based Automated clustering of digital dental X-ray images is introduced in Matlab 2018 with the key interface shown below in Fig Displays the segmented data for Otsu filter, FCM and GOMB-FCM performance.

4.4 Comparison of Cluster validity indices and its performance measures

This paper illustrates the comparison of the various cluster validity indices of proposed GOMB-FCM and the existing FCM, EA-FCM, FCM-SC based on 500 dental image data sets. The accuracy of various methods is measured based on the various cluster validity indices (CVI) for the different number of clusters shown in the below figure.

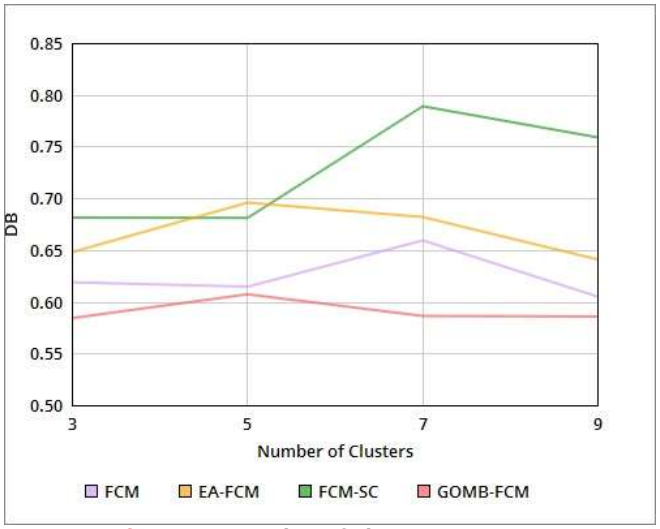

Figure 4.6: Number of Clusters Vs CVI-DB

Table 4.1: Performance measures with cluster K=2

For K = 2	FCM	eSFCM	SSFC-SC	SSFC-SGOM
DB	0.6152	0.618	0.7675	0.6032
BR	-119510	-135760	-48569	-25289
PBM	21434	21202	11553	2589.8
IFV	6.0026	662.1102	15.1216	15.5166
BH	3883.3	3792.1	4347.6	4763.8
VRC	509820000	531510000	371360000	373020000
TRA	137720000	136740000	154700000	195570000
TTI	137720000	136740000	154700000	195570000
TWI	108070	115470	57309	66293

The number of Clusters Vs CVI-DB for proposed and existing methods are shown in Figure: 4.6. The range of DB value is between 0 and 1. The graph shows that the DB value of proposed algorithm is minimum when compared to the existing methods. The lower DB value shows the better separation of clusters and the closeness inside the cluster.

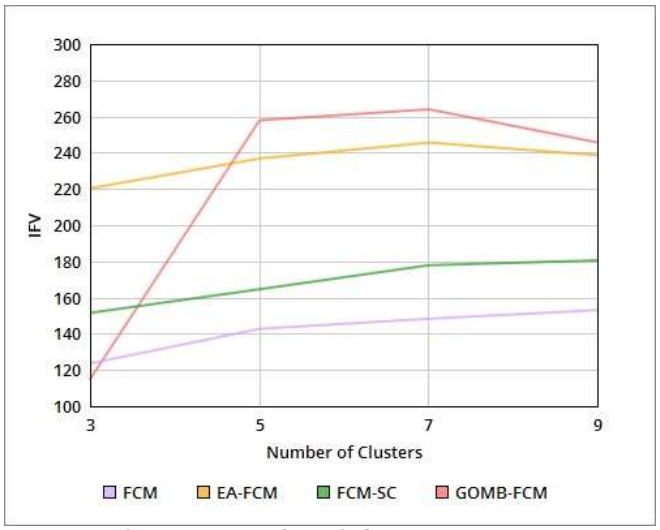

Figure 4.7: Number of Clusters Vs CVI-IFV

The number of Clusters Vs CVI-IFV for proposed and existing methods shown in Figure: 4.7. The IFV curve of proposed algorithm tends to increase with the number of clusters as well, it has a wave crest at the number of cluster 7, beyond that it reduces. The IFV include intra-cluster comparability and inter-cluster difference which reflect the partition of Fuzzy Clustering. The comparability of intra-cluster reflects the measurement of separation between each spatial object and the cluster centre within a cluster. The inter-cluster variation shows the measurement of separation between the centre of clusters. The ratio of inter-clusters to intra-clusters can reflect the partition results. A higher of

IFV shows better clustering. The proposed work has produced better segmentation.

Table 4.2: Performance measures with cluster K=5

For K = 5	FCM	eSFCM	SSFC-SC	SSFC-SGOM
DB	0.6072	0.6958	0.681	0.64503
BR	-142900	-133550	-120580	-102350
PBM	81351	71960	63086	84794
IFV	42.7252	3266.8	114.6023	3347.9
BH	532.5606	577.0462	606.7311	2400.4
VRC	401800000	392860000	341860000	373860000
TRA	18662000	19937000	20414000	63757000
TTI	18662000	19937000	20414000	63757000
TWI	205280	189930	178320	198633

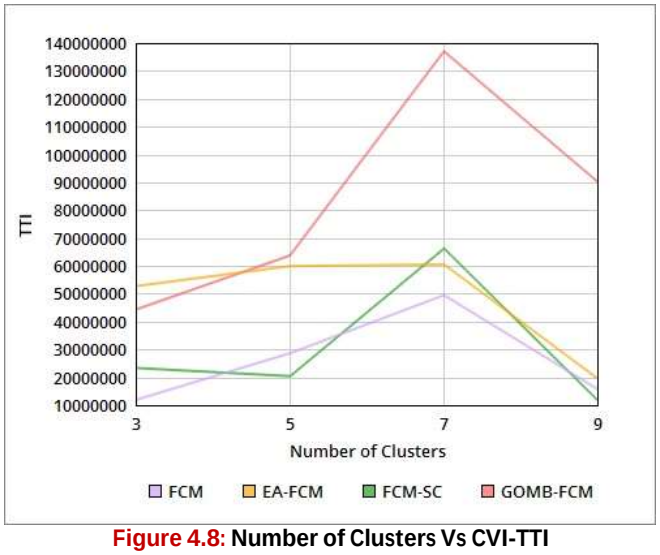

Figure 4.8: Number of Clusters Vs CVI-TTI

The number of Clusters Vs CVI-TTI for proposed and existing methods shown in Figure: 4.8. The TTI curve of the proposed algorithm be likely to move up with the number of clusters as well, it strikes the highest point at the number of cluster 7, after that it reduces.

Table 4.3: Performance measures with cluster K=10

For K = 10	FCM	eSFCM	SSFC-SC	SSFC-SGOM
DB	0.582	0.6495	1.0314	0.9035
BR	-214420	-239540	-153990	-90696
PBM	103780	93365	28858	9313.6
IFV	53.9486	Inf	124.5507	141.514
BH	154.8359	173.3436	299.9956	2208.4
VRC	38000000	379000000	375000000	384810000
TRA	4578100	5005900	15788000	42473000
TTI	4578100	5005900	15788000	42473000
TWI	364590	332400	101090	135813

CONCLUSION

In this paper, a new segmentation algorithm was proposed for dental X-ray image based on spatial information fuzzy C means algorithm called Gradient Orientation Mapping Based Semi-Supervised Fuzzy Clustering (GOBM-FCM). In this proposed method along with the Fuzzy C-Mean clustering additional features extracted from the dental X-ray images were used. Through the experiments in the dental X-ray image, the proposed GOBM-FCM algorithm obtains better performance measures than other FCM algorithm. Because of the usage of these features, the various parts of the dental image such as the fine edges of the teeth, enamel and pulp, gum areas, infected dental areas were segmented effectively. Various cluster validity indices are

measured and the performance of the system is analysed. From the CVI it is noted that the proposed algorithm produces better-segmented results for the number of cluster 10. The results demonstrate that the performance of proposed GOMB-FCM algorithm segmentation is better than the state-of-the-art algorithms. Further work will include the proposed work for the 3D image. Classification of different dental diseases from the digital X-ray image will be investigated further.

CONFLICT OF INTEREST

None

REFERENCES

1. Qingyong Li , Min Zheng, Feng Li, Jianzhu Wang, Yangli-AoGeng, Haibo Jiang, Retinal Image Segmentation Using Double-Scale Non-Linear Thresholding On Vessel Support Regions, Caai Transactions On Intelligence Technology, 2017, Vol. 2, Iss. 3, Pp. 109–115.
2. Ronghua Shang, Yijing Yuan, Licheng Jiao, Biao Hou, Member, Amir MasoudGhalamzanEsfahani, And RustamStolkin, Fast Algorithm For Sar Image Segmentation Based On Key Pixels,2017, IEEE Journal Of Applied Earth Observations And Remote Sensing,2017, Vol.10, Iss.12, Pp-5657-5673.
3. LiyileiSu,XianjunF, Xiaodong Zhang, Xiaoguang Cheng, Yimin Ma, YungenGan, And Qingmao, Hudelineation Of Carpal Bones From Hand X-Ray Images Through Prior Model, And Integration Of Region-Based And Boundary-Based Segmentations, IEEE Access,2017, Vol.6, Pp-19993-20008.
4. Hong Huang, FanzhiMeng, Shaohua Zhou, Feng Jiang, And GunasekaranManogaran, Image Segmentation Based On Fcm Clustering Algorithm And Rough Set, Ieee Access, Special Section On New Trends In Signal Processing And Analysis,2019, Vol.7, Pp-12386-12396.
5. Mohammed Khammari, Robust Face Anti-Spoofing Using Cnn With Lbp And Wld, IET Image Processing, 2019, Vol. 13 Iss. 11, Pp. 1880-1884.
6. Jianhua Song, and Zhe Zhang, A Modified Robust FCM Model with Spatial Constraints for MR Image Segmentation, Information, MDPI 2019, Vol.24, Iss:10, PP-1-15.
7. JiaZheng, Dinghua Zhang, Kuidong Huang, YuanxiSun, Adaptive image segmentation method based on the fuzzy c-means with spatial information IET Image Process., 2018, Vol. 12 Iss. 5, pp. 785-792.
8. Tao Lei, XiaohongJia, Yanning Zhang, Shigang Liu, HongyingMeng, And Asoke K. Nandi, Superpixel-Based Fast Fuzzy C-Means Clustering For Color Image Segmentation IEEE Transactions On Fuzzy Systems, Vol: 27, Iss: 9, Sept. 2019, pp- 1753 – 1766
9. Huabin Wang, Mengli Du, Jian Zhou, And Liang Tao, Weber Local Descriptors with Variable Curvature Gabors Filter for Finger Vein Recognition, IEEE Access, Vol: 7, Iss: 9, July 2019, pp- 108261 - 108277
10. Zhenjiang Gong, Guangqiang Li, Yongju Zhang, Changdi Li, Lei Yu, Application of static gesture segmentation based on an improved canny operator, The Journal of Eng., 2019, Vol: Iss. 15, pp. 543-546
11. Yuli Chen, Yide Ma, Dong Hwan Kim, and Sung-Kee Park, Region-Based Object Recognition by Color Segmentation Using a Simplified Pcnn , IEEE Transactions On Neural Networks And Learning Systems, Vol. 26, No. 8, August 2015
12. R. Suresh, A. Nagaraja Rao, B. Eswara Reddy Detection and classification of normal and abnormal patterns in mammograms using deep neural network, Concurrency Computation PractExper. , John Wiley & Sons, Ltd., Special Issue, 2019,
13. Dongdong Cheng, Qingsheng Zhu, Jinlong Huang, Quanwang Wu, and Lijun Yang, A Novel Cluster Validity Index Based on Local Cores, IEEE Transactions On Neural Networks And Learning Systems, VOL. 30, ISS. 4, AUGUST 2015,PP- 985-999.
14. Abraham B, Weng G, Ong M, Attarwala AA, Molina F, Büsing K, GlattingG, Comparison of five cluster validity indices performance in FET-PET image segmentation using k-means., Medical Physics,2017, Vol:44, Issue:1, PP:209-220.
15. Fariza, Arna, Agus Zainal Arifin, EhaRenwiAstuti, and Takio Kurita. "Segmenting Tooth Components in Dental X-Ray Images Using Gaussian Kernel-Based Conditional Spatial Fuzzy C-Means Clustering Algorithm."
16. Ali, Mumtaz, Mohsin Khan, and Nguyen Thanh Tung. "Segmentation of dental X-ray images in medical imaging using neutrosophic orthogonal matrices." Expert Systems with Applications 91 (2018): 434-441.
17. Said, Eyad, Gamal F. Fahmy, DiaaNassar, and Hany Ammar. "Dental x-ray image segmentation." In Biometric Technology for Human Identification, vol. 5404, pp. 409-417. International Society for Optics and Photonics, 2004.
18. Kumar, Anuj, H. S. Bhadauria, and Annapurna Singh. "Semi-supervised OTSU based hyperbolic tangent Gaussian kernel fuzzy C-mean clustering for dental radiographs segmentation." Multimedia Tools and Applications 79, no. 3 (2020): 2745-2768.
19. Karthick, G., and R. Harikumar. "Comparative Performance Analysis of Naive Bayes and SVM classifier for Oral X-ray images." In 2017 4th International Conference on Electronics and Communication Systems (ICECS), pp. 88-92. IEEE, 2017.
20. Modi, Chintan K., and Nirav P. Desai. "A simple and novel algorithm for automatic selection of ROI for dental radiograph segmentation." In 2011 24th Canadian Conference on Electrical and Computer Engineering (CCECE), pp. 000504-000507. IEEE, 2011.
21. Jain, Kavindra R., and N. C. Chauhan. "Clustering Techniques for Dental Image Analysis." In Dental Image Analysis for Disease Diagnosis, pp. 103-128. Springer, Cham, 2019.
22. Al-Ayyoub, Mahmoud, ShadiAlZu'bi, YaserJararweh, Mohammed A. Shehab, and Brij B. Gupta.

"Accelerating 3D medical volume segmentation using GPUs." Multimedia Tools and Applications 77, no. 4 (2018): 4939-4958.
23. Fariza, Arna, Agus Zainal Arifin, and EhaRenwiAstuti. "Interactive Segmentation of Conditional Spatial FCM with Gaussian Kernel-Based for Panoramic Radiography." In 2018 International Symposium on Advanced Intelligent Informatics (SAIN), pp. 157-161. IEEE, 2018.
24. Kumar, Rajesh, Rajeev Srivastava, and Subodh Srivastava. "Detection and classification of cancer from microscopic biopsy images using clinically significant and biologically interpretable features." Journal of medical engineering 2015 (2015).
25. Lin, Kuo-Ping, Hao-Feng Chang, Tung-Lian Chen, Yu-Ming Lu, and Ching-Hsin Wang. "Intuitionistic fuzzy C-regression by using least squares support vector regression." Expert Systems with Applications 64 (2016): 296-304.
26. Buhari, M. P. A., and S. K. Mohideen. "A combination of fuzzy positioned dental X-ray analysis model to presume the peculiar images." International Journal of Computers and Applications 42, no. 1 (2020): 17-22.
27. Poornima, D., and Asha Gowda Karegowda. "A Review of Image Segmentation Techniques Applied to Medical Images." International Journal of Data Mining And Emerging Technologies 8, no. 1 (2018): 78-94.
28. Zhang, Yanbo, Ying Chu, and Hengyong Yu. "Reduction of metal artifacts in x-ray CT images using a convolutional neural network." In Developments in X-Ray Tomography XI, vol. 10391, p. 103910V. International Society for Optics and Photonics, 2017.
29. Krishan, Abhay, and Deepti Mittal. "Effective segmentation and classification of the tumour on liver MRI and CT images using multi-kernel K-means clustering." Biomedical Engineering/BiomedizinischeTechnik (2019).
30. Divya, KrishnappaVeena, AnandJatti, P. Revan Joshi, and S. Deepu Krishna. "A Correlative Study of Contrary Image Segmentation Methods Appending Dental Panoramic X-ray Images to Detect Jawbone Disorders." In Progress in Advanced Computing and Intelligent Engineering, pp. 25-35. Springer, Singapore, 2019.
31. Wang, Ching-Wei, Cheng-Ta Huang, Jia-Hong Lee, Chung-Hsing Li, Sheng-Wei Chang, Ming-JhihSiao, Tat-Ming Lai et al. "A benchmark for comparison of dental radiography analysis algorithms." Medical image analysis 31 (2016): 63-76.
32. Tom, Christy Elezabath, and Jerin Thomas. "Segmentation of Tooth and Pulp from Dental Radiographs." International Journal of Scientific & Engineering Research 6, no. 11 (2015): 115-121.
33. Mekky, Nagham E., E-Z. Fatma, and SherifKishk. "A new dental panoramic X-ray image registration technique using hybrid and hierarchical strategies." The 2010 International Conference on Computer Engineering & Systems, pp. 361-367. IEEE, 2010.
34. Sridhar, Bitra, and DandeyVenkata Prasad. "Finding 3D Teeth Positions by Using 2D Uncalibrated Dental X-Ray Images." (2010).
35. Gan, Yangzhou, Ziyang Xia, Jing Xiong, Qunfei Zhao, Ying Hu, and Jianwei Zhang. "Toward accurate tooth segmentation from computed tomography images using a hybrid level set model." Medical Physics 42, no. 1 (2015): 14-27.

Cite this article: Peer Ahamed Buhari. M Gradient Orientation Mapping Based Fuzzy C – Means Clustering for Digital Dental X – Ray Images. J. Cardiovascular Disease Res. 2020; 11 (2): 96 – 108